Angular distributions in autodetachment from doubly excited O- states

Dahl, P.; Andersen, T.; Jodal, L.; Kylstra, N.J.; Hansen, J.E.; Vaeck, N.

Published in:
Physical Review A

DOI:
10.1103/PhysRevA.48.2844

Angular distributions in autodetachment from doubly excited O^- states

P. Dahl, T. Andersen, and L. Jødal
Institute of Physics and Astronomy, Aarhus University, DK-8000 Aarhus C, Denmark

N. J. Kylstra, J. E. Hansen, and N. Vaeck
van der Waals-Zeeman Laboratory, University of Amsterdam, Valckenierstraat 65, NL-1018 XE Amsterdam, The Netherlands
(Received 22 March 1993)

The angular distributions of electrons ejected from collisionally excited O^- ions have been measured in order to test the previous assignments of excited states for this ion. The angular distributions support the interpretation that the two dominant peaks in the electron-energy spectrum represent the autodetachment of the $2p^3(^2D)3s^2\,^2D^o$ state, decaying to the ^3P and ^1D states of the oxygen ground-state configuration, with an experimental branching ratio of 1.58 ± 0.08, and not that two different autodetaching states are populated, as previously assumed. Theoretical calculations are in good agreement with the experimental findings.

PACS number(s): 32.80.Dz, 34.50.Fa, 31.20.Tz

I. INTRODUCTION

Autodetaching doubly excited states of negative atomic ions are known to exist for several elements, but information about the properties of such states in simple negative ions is still very limited due to the lack of selective excitation techniques (for recent reviews, see Refs. [1–3]). In recent years, the selectivity of low-energy ion-atom collisions, however, has been exploited successfully to study doubly excited states in the halogen ions F^- [4,5], and Cl^- [6,7]. It was clearly demonstrated [4–7] that only one doubly excited state or states belonging to the same configuration of the ion were populated, in contrast to the findings of earlier studies [8,9], but also that the doubly excited state decayed by autoionization to states belonging to different configurations in the neutral atom. The doubly excited states in negative ions populated by low-energy ion-atom or ion-molecule collisions may be classified as belonging to configurations of (positive-core) nl^2 or (positive-core) $nln'l'$, with the lowest available ns^2 representing the favored configuration [8]. The halogen ions F^- and Cl^- are representative for the ns^2 type and C^- for the $nsnp$ type [8]. A notable exception, however, is O^-, for which a $2s2p^6$ subshell excitation has been claimed to exist, in addition to the expected $2p^3(^2D)3s^2$ excitation. These two excited states have been proposed [9] to explain the origin of the dominant peaks present in the experimental electron spectrum (see Fig. 1). The $2s2p^6\,^2S$ state was assigned to the resonance line located just above 10 eV, the $2p^3(^2D)3s^2\,^2D^o$ state to the line at 12 eV. These assignments were supported by electron-scattering experiments [10] on atomic O and by theoretical calculations of the energy positions [11,12]. The recent findings for the halogen systems [4–7], however, lie behind the present reinvestigation of the O^- system.

The original interpretation by Edwards and Cunningham [9] of the origin of the two resonances in O^- was based on the population of the two excited states, $2p^3(^2D)3s^2\,^2D^o$ and $2s2p^6\,^2S$, in O^-, which should be nearly degenerate in energy and decay as follows (proposal I):

$$O^-2p^3(^2D)3s^2\,^2D^o \rightarrow O2p^4\,^3P+\epsilon p \quad 12\ \text{eV}\ ,$$

$$O^-2s2p^6\,^2S \rightarrow O2p^4\,^1D+\epsilon d \quad 10\ \text{eV}\ .$$

An important point in favor of this proposal was that the energy difference between the two peaks had been measured to be 2.01(2) eV and not 1.97 eV, which is the ^3P-^1D splitting in the oxygen ground-state configuration. The energy-difference measurement eliminated the proposal (II) that the two resonances could represent the branching between autodetachment decays of the same doubly excited O^- state:

$$O^-2p^3(^2D)3s^2\,^2D^o \rightarrow \begin{cases} O2p^4\,^3P+\epsilon p & 12\ \text{eV} \\ O2p^4\,^1D+\epsilon p & 10\ \text{eV}\ . \end{cases}$$

An third proposal (III) could have been that proposal I is correct, but that the 10-eV peak represents a superposi-

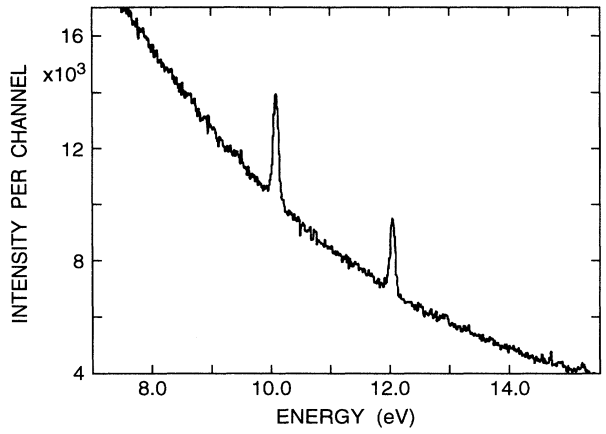

FIG 1. Electron spectrum from 7-keV O^--He collisions.

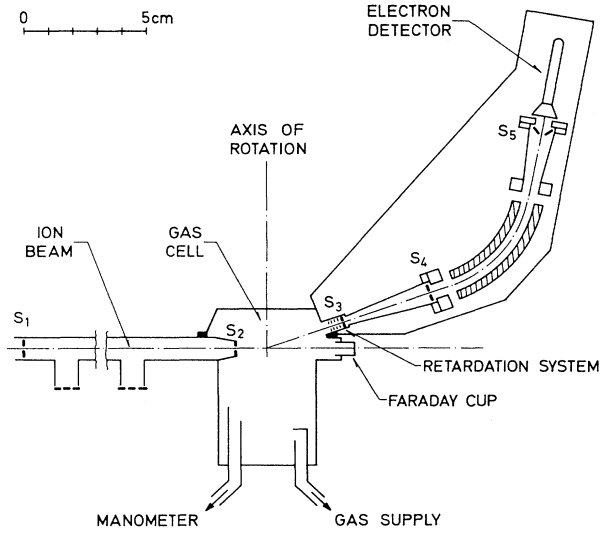

FIG. 2. Diagram of the apparatus. The analyzer and detector can rotate through 360°, thus allowing the electron to be detected from 20° and 160°. The ion beam is collimated by S_1 and S_2; the perpendicular apertures S_3 and S_4 collimate the electron beam before the analyzer. Retardation may be applied with the electron collimator and analyzing system at a negative potential.

tion of two peaks, so that the following decay channel is also active:

$$O^-2p^3(^2D)3s^2\,^2D^o \rightarrow O2p^4\,^1D + \epsilon p \quad 10 \text{ eV} .$$

A reinvestigation of the O^- system was further stimulated by the fact that the electron affinity of the $2s2p^6\,^2S$ state as a consequence of proposal I would be as large as 3.6 eV with respect to the $2s2p^5\,^3P^o$ state in neutral oxygen, whereas the electron affinity [13] is only 1.46 eV for the ground-state of O^- and 0.46 eV for the $2p^3(^2D)3s^2\,^2D^o$ state, respectively.

We have performed a combined experimental and theoretical investigation of the three proposals. Preliminary theoretical calculations on the autodetachment rates of the $2p^3(^2D)3s^2\,^2D^o$ term to the ^3P and ^1D terms in the $2p^4$ ground-state configuration supported proposal II. However, these results were not entirely conclusive on their own, prompting the measurement of the angular dependences of the emitted electrons, since no angular dependence is expected from the ^2S in contrast to the $^2D^o$ resonance. The observed angular distributions are compared with theoretical predictions.

II. EXPERIMENTAL TECHNIQUE

The mass-separated O^- beams with energies ranging from 1 to 25 keV were obtained from accelerators of the isotope-separator type, equipped with a sputter ion source operating with Cs deposition on the surface. Excitation is obtained by collisions in a helium-gas target. The electron spectrometer used was originally described by Dahl *et al.* [14]. Figure 2 presents the essential parts of the instrument. The relative energy resolution at full width at half maximum (FWHM) is 1.8% and the product of the solid angle and observed beam length is $1.8\times10^{-4}/\sin\theta$ sr cm. The energy resolution may be improved by means of preretardation. For an analyzer potential $V_A<0$, the electron energy E is lowered to $E_A=E+eV_A$ and, with a deflection voltage ΔV, electrons are detected for $E_A=ke\Delta V$, where k is the spectrometer constant. An energy spectrum may be recorded by varying V_A, while ΔV and thus E_A are fixed. The constant k may be determined with a high accuracy by recording a spectrum with a sharp peak E_0 for different values of ΔV. The relation between the peak position V_A and the deflection voltage ΔV is $ke\Delta V=E_0+eV_A$, so that k is the slope of the curve for V_A vs ΔV. The constant k was determined to be 5.10 ± 0.02, allowing us to determine the energy separation between the two dominant resonances within an accuracy of 0.01 eV. The results for the angular distributions have been obtained from the peak intensities measured without using preretardation.

III. THEORETICAL APPROACH

A. Multiconfiguration Hartree-Fock

An important factor behind the present reinvestigation of the O^- decay scheme was the early results obtained using the configuration interaction Hartree-Fock (HF) program of Cowan [15] on the autodetachment rates of the $2p^3(^2D)3s^2\,^2D^o$ term to the ^3P and ^1D terms in the $2p^4$ ground-state configuration. The calculated branching ratio between the two decay channels supported, as already mentioned, proposal II. To confirm this result, which was obtained using very restricted expansions, more extensive multiconfiguration Hartree-Fock (MCHF) calculations were carried out.

In the MCHF approach, the wave functions of the autodetaching state and of the two bound states, in which the neutral atom is found after the decay, are written as linear combinations of configuration state functions (CSF's),

$$|\Psi(LS)\rangle = c_0|\Phi(\gamma_0 LS)\rangle + \sum_{\alpha,r} c_\alpha^r|\Phi(\gamma_\alpha^r LS)\rangle + \sum_{\alpha,\beta,r,s} c_{\alpha\beta}^{rs}|\Phi(\gamma_{\alpha\beta}^{r,s}LS)\rangle ,$$

where $|\Phi(\gamma_0 LS)\rangle$ is the reference function and $|\Phi(\gamma_\alpha^r LS)\rangle$ is a singly excited CSF consisting of an excitation of an electron from the orbital α to the orbital r; similarly, $|\Phi(\gamma_{\alpha\beta}^{rs}LS)\rangle$ is a doubly excited CSF, and c is a unit vector. Using such an expansion, a continuum state can be presented as

$$|\Psi(L'S')\phi_{\epsilon l},LS\rangle = c_0|\Phi(\gamma_0 L'S')\phi_{\epsilon l},LS\rangle + \sum_{\alpha,r} c_\alpha^r|\Phi(\gamma_\alpha^r L'S')\phi_{\epsilon l},LS\rangle + \sum_{\alpha,\beta,r,s} c_{\alpha\beta}^{rs}|\Phi(\gamma_{\alpha\beta}^{rs}L'S')\Phi_{\epsilon l},LS\rangle,$$

where the final bound-state wave function is $|\Psi(L'S')\rangle$ and $|\phi_{\epsilon l}\rangle$ is the continuum electron wave function.

The continuum wave functions were determined using the program MCHF_AUTO developed by Froese Fischer and Brage [16]. This program, which was designed as part of the MCHF atomic-structure package [17], solves the radial Schrödinger equation of the continuum electron in the field of the final bound state of the neutral atom and calculates the Coulomb interaction between the continuum state and the autodetaching state. The autodetachment rates are then determined using Fermi's "golden rule." An important constraint is that the program requires orthogonality between the CSF's of the autodetaching and final bound states, and therefore a common orbital basis set for all three states must be used. In order to construct a basis set that adequately describes the three states, the set should contain orbitals specifically optimized on each of the individual terms. Moreover, since such a common basis set can lead to prohibitively large configuration-interaction (CI) expansions, care must be taken to construct the basis in the most efficient manner. An obvious way to do this is by observing the changes in energy and autoionization rates upon the addition of each new orbital. The number of orbitals optimized on each state can then be varied so that only the important orbitals are included in the basis set.

The basis set was constructed as follows. The orbitals $\{1s,2s,2p,3s\}$ were taken to be the HF radial functions for the $2p^3(^2D)3s^2\,^2D^o$ state. Using the MCHF program of Froese Fischer [18], four series of virtual orbitals with $l=s$, p, d, and f were obtained. Each series was constructed independently. Orbitals were optimized on a MCHF expansion that consisted of all CSF's corresponding to single and double excitations to the set of virtual orbitals with a particular l value including the orbital to be optimized. It was found that for each orbital optimized on $^2D^o$, one optimized on alternately ^3P and ^1D resulted in the best representation. We compared the correlation between the s and p series obtained in this way with a more limited basis set expansion determined from CSF's that contained excitations to both s and p virtual orbitals and found the correlation to be adequately represented.

TABLE I. Comparison between calculated and measured energy differences in the negative-oxygen-ion–oxygen-atom system.

	Calculated (eV)	Experiment (eV)
$O^-(^2D^o)$-$O(^3P)$	12.00	12.08(5)
$O^-(^2D^o)$-$O(^1D)$	9.93	10.11(5)
$O(^1D)$-$O(^3P)$[a]	2.07	1.97(1)

[a]Observed value [21] 1.967.

The final basis consisted of the orbitals $\{1s,2s,3s,4s,5s,2p,3p,4p,5p,6p,3d,4f\}$, and the final wave functions were obtained by CI calculations including single and double excitations, excluding excitations from the $1s$ orbital, to all the virtual orbitals above. The CI expansions of the states $^2D^o$, ^3P, and ^1D consisted of about 800, 400, and 300 CFS's, respectively, where approximately a third of all possible CSF's was eliminated due to a negligible contribution to the expansions. The MCHF energy separations between the different states are given in Table I and compared with the experimental values. Autodetachment rates for the $^2D^o \rightarrow {}^1D$ and the $^2D^o \rightarrow {}^3P$ channels were calculated to be 6.3×10^{-4} eV and 4.7×10^{-4} eV, respectively, yielding a branching ratio of 1.3 with an estimated error of $\pm 20\%$. The error limit is determined from the variation observed in the ratio during the construction of the orbital basis. The results assume that only ϵp electrons are emitted and thus that the emission of ϵf electrons is negligible. The Coulomb interaction between the HF states representing the autodetaching $2p^3(^2D)3s^2\,^2D^o$ state and the $2p^4(^3P,^1D)\epsilon f\,^2D^o$ continuum states is zero, so that an ϵf contribution to the autoionization rates is possible only in higher-order interactions. In fact, it was not possible to bind an f wave on either of the final bound MCHF states with the MCHF_AUTO program, and the weakness of the interaction was verified with a limited CI expansion using the Cowan program [15].

We also performed MCHF calculations in an attempt to determine the position of the $2s2p^6\,^2S$ state. These calculations appeared less reliable than the ones above and convergence problems were experienced. Moreover, the energy of this state appeared to be extremely sensitive to the choice of basis set.

B. Angular distributions

The branching ratio obtained in the MCHF calculations was in good accord with proposal II, as discussed in the next section. However, we realized that it could be underpinned by considering the angular distribution of the emitted electrons. A considerable amount of work has been done to elucidate the dependence of angular distributions on the quantum numbers of the states involved

[19], but, to our knowledge, the angular dependences of the individual branches of a complex decay have not been used to identify the decay scheme before.

In order to derive an expression for the angular distribution of the autodetaching electrons, the following assumptions are made: (i) The excitation of the negative ion and its subsequent decay via autodetachment can be treated as a two-step process. Thus the lifetime of the autodetaching state must be much longer than characteristic interaction times between the helium target and the projectile, so that the decay process is not influenced by the excitation process and vice versa. This requirement is fulfilled in the experiments. (ii) The collision process involves no momentum transfer, only excitation and alignment of the ion. Thus the collision process defines a preferred direction in space which will be taken to be the quantization axis. (iii) It is assumed that the fine-structure splitting of the excited state is considerably larger than the autoionization widths, so that the states are appropriately characterized by *LSJM* coupling. An upper bound for the fine-structure splitting is given by the observed splitting of the parent term in O^+. From our calculated widths, it follows that this requirement is met. (iv) The recoil momentum of the ejected electron can be neglected. Implicitly it is assumed that the decay process can be treated adequately using time-dependent first-order perturbation theory. More complete discussions can be found in [19].

Taking θ to be the angle between the outgoing electron and the quantization axis, the following general formula for the relative intensity can be written:

$$I(\theta)=\frac{\pi}{\hbar}C\sum_a p(i\rightarrow a)\sum_f |\langle a|V|f\rangle|^2 .$$

The initial state, i.e., the ground state of the negative ion, is written as i, the autoionizing state as a, and the final continuum state as f. The factors $p(i\rightarrow a)$ are the population probabilities which give the relative population of the magnetic substates in a. In the evaluation of the sums above, an average is performed over unresolved angular-momentum states of the autodetaching state a, while the undetermined angular-momentum and spin states of the final state f are summed over. The constant C is defined so that integration over θ yields the total autoionization rate. The general procedure is to express the final state as an antisymmetrized wave function consisting of the bound state of the neutral atom and a plane-wave expansion for the ejected electron. The interaction above is then written as an expansion over the reduced Coulomb matrix elements of the *LS* coupled states [19]. Assuming that the population probabilities are spin independent, the expression for the angular dependence is, following the notation of Mehlhorn and Taulbjerg [19],

$$I(\theta)=\frac{\pi}{\hbar}C\sum_{k=0}^{L}\rho_{2k0}(LL)\sum_{l,l'}F_{2k}(ll')R_{ll'}D_{2k}P_{2k}(\cos\theta) ,$$

with

$$\rho_{k0}(LL)=\sum_{M_L\geq 0}(2-\delta_{M_L0})\rho_{M_LM_L}(-1)^{k-L-M_L}(2k+1)^{1/2}\times\begin{pmatrix} L & L & k\\ -M_L & M_L & 0\end{pmatrix},$$

$$F_k(ll')=(-1)^{L+L_f}(2l+1)^{1/2}(2l'+1)^{1/2}\times(2k+1)^{1/2}(2L+1)\times\begin{pmatrix} l & l' & k\\ 0 & 0 & 0\end{pmatrix}\begin{Bmatrix} L & L & k\\ l & l' & L_f\end{Bmatrix},$$

$$R_{ll'}=\langle\alpha_fL_fl,L\|V\|\alpha L\rangle\langle\alpha L\|V\|\alpha_fL_fl',L\rangle ,$$

and

$$D_k=\sum_J\frac{(2J+1)^2}{2S+1}\begin{Bmatrix} J & J & k\\ L & L & S\end{Bmatrix}^2 .$$

The autodetaching state is coupled to *LSJM* while L_fS_f is the symmetry of the final bound state. The $P_k(\cos\theta)$ are the Legendre polynomials. In the density-matrix formalism employed above, the population probabilities are the diagonal elements of the density matrix, $\rho_{M_LM_L}$, while the angular distribution is written in terms of the irreducible components of the density matrix, the state multipoles $\rho_{kq}(LL)$ [20]. Only the state multipoles of even rank and $q=0$ appear in the expression, reflecting the symmetry about $\theta=\pi/2$ and the axial symmetry, respectively, of the system [20]. When the population probabilities are equal, the angular distribution is isotropic, and when only one partial wave contributes, the expression for the angular intensity is proportional to the autoionization rate.

For the autoionization process

$$2p^3(^2D)3s^2\,^2D^o\rightarrow 2p^4(^3P,^1D)+\epsilon p ,$$

the formula above reduces to

$$I(\theta)=\frac{1}{\hbar}\Gamma^{(\pm)}[1\pm\Delta P_2(\cos\theta)] ,$$

where Γ is the autoionization halfwidth, the plus and the minus signs correspond to the ^3P and the ^1D state, respectively, and

$$\Delta=\tfrac{19}{25}(\rho_{00}+\rho_{11}-2\rho_{22}) .$$

Since the branching ratio was calculated to be approximately 1:1, the angular dependences are expected to be, aside from a constant background, roughly mirror images of each other. In contrast, the decay

$$2s2p^6\,^2S\rightarrow 2p^4\,^1D+\epsilon d$$

contains no angular dependence.

IV. RESULTS AND DISCUSSION

The energy separation between the two intense resonance peaks in Fig. 1 was determined to be 1.97 ± 0.01 eV, with the lower energy peak located at 10.11 ± 0.05 eV on the absolute scale. This energy difference deviates

slightly from the 2.01 eV claimed by Edwards and Cunningham [9] but is consistent with the energy separation between the ^1D and ^3P states in the oxygen ground-state configuration [21]. The intensity ratio between the two peaks observed at 20° was measured at impact energies ranging from 2 to 20 keV and found to be constant within an experimental accuracy of ~10%. [We note that Edwards reported a different behavior in a private communication to Ref. [11], (although this point is not mentioned in the final paper [9]). This result provided additional motivation for the original dismissal of proposal II.] At 2 keV, the electron peaks are a factor of two larger than the underlying background, originating from collisional detachment of the O^- ion, whereas at 20 keV, the peaks account for only a minor fraction (~15%) of the background signal. Also, the widths of the electron peaks were independent of impact energy. If proposal I is correct, and two different excited states are populated, the populations are expected to be strongly dependent on collision velocity, particularly since the production of states of the type $2p^3 3s^2$ is expected to dominate completely at low collision velocities [22]. The fact that no such dependence is observed is a strong indication that only one state is populated. Similarly, the fact that the linewidths remain constant makes it unlikely that a second state contributes to the 10-eV peak (proposal III).

The angular dependences of electrons emitted from the two dominating resonances in Fig. 1 are presented in Fig. 3. Experimentally, it is the double-differential cross sections which are measured. These cross sections are, using assumption (ii), proportional to the total excitation cross section. Thus it is possible only to extract the branching ratio from the angular data since the excitation cross section is unknown. The curves in Fig. 3 represent least-squares fits to the data, using the theoretical form of the angular-distribution functions. These expressions assume ϵp electron emission only. The two angular distributions are mirror images of each other, with the branching ratio determined as 1.58±0.08. The error limit given represents the sum of statistical and systematic errors, with each assumed to account for roughly 50% of the total error. The angular-distribution measurements completely eliminate the possibility for assigning one of the resonance peaks to a ^2S resonance. Thus proposal I can be dismissed on these grounds. This conclusion is also consistent with estimates of the $2p^3(^2D)3s^2\,^2D^o - 2s2p^6\,^2S$ energy difference in O^-. As mentioned above, it is difficult to calculate the position of the $2s2p^6\,^2S$ term in O^-. Our MCHF calculations indicate that the term is not (or weakly) bound relative to the $2s2p^5\,^3P^o$ term in O, while isoelectronic estimates, although rather unreliable since the position of the term is unknown in F [23], indicate an electron affinity of less than 2.5 eV, which should be compared to the value of 3.6 eV associated with proposal I. Chase and Kelly [12] calculated an affinity of 3 eV but this calculation was directed towards the determination of the photodetachment cross section, and Kelly indicated in a private communication [9] that an error of 0.6 eV in the calculated electron affinity was possible.

The theoretical branching ratio for the decays of the

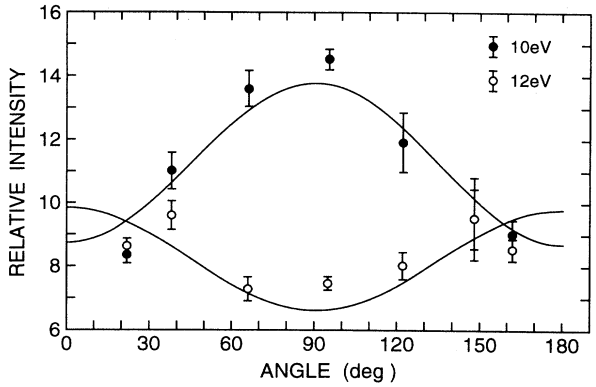

FIG. 3. Angular distributions of autodetaching electrons from the doubly excited $2p^3(^2D)3s^2\,^2D^o$ state in O^-. The curves represent least-squares fits of the expressions for the theoretical angular distribution (see text) to the experimental data points.

$2p^3(^2D)3s^2\,^2D^o$ state to the ^3P and ^1D states in the oxygen ground-state configuration is, as mentioned, equal to 1.3±20%, only slightly lower than the experimental value of 1.58±0.08. The good agreement is a further indication that it is unlikely, as assumed in proposal III, that the 10-eV resonance peak could represent a superposition of two decay channels. The extra structure present in the experimental data (particularly at 20° and 160°) could suggest that the $^2D^o$ state may be emitting f electrons in addition to the p electrons. However, the data cannot be better fitted using angular expressions for a decay with both p and f partial waves. This is consistent with the fact that the probability for decay via an f wave is very small, as mentioned above.

V. CONCLUSION

We conclude that all the experimental and theoretical data support proposal II, which is based on the population of only the $2p^3(^2D)3s^2\,^2D^o$ doubly excited state in O^-, followed by a branching between two autodetaching decay channels, leading to the ^3P and ^1D states, respectively, of the $2p^4$ ground-state configuration of oxygen. The branching ratio for these decays is ~1.6, in agreement with the theoretical prediction, while Edwards and Cunningham [9] estimated a branching ratio of >20 on the basis of their acceptance of proposal I. Correct estimates of branching ratios for autoionization processes in atoms isoelectronic or homologous with O^-, such as the neutral halogen atoms, may be a significant help in identifying the rather complicated electron spectra recently observed from collisional excitation of atomic chlorine [7] or from two electron-excitation processes in synchrotron-radiated chlorine [24].

ACKNOWLEDGMENTS

We would like to thank Dr. C. Froese Fischer and Dr. T. Brage for putting the MCHF_AUTO program at our disposal.

[1] V. A. Esaulov, Ann. Phys. (Paris) **11**, 493 (1986).
[2] T. Andersen, Phys. Scr. **T34**, 23 (1991).
[3] D. R. Bates, Adv. At. Mol. Phys. **27**, 1 (1991).
[4] J. P. Grouard, V. A. Esaulov, R. I. Hall, J. L. Montmagnon, and Tuan Vu Ngoc, J. Phys. B **19**, 1483 (1986).
[5] J. Poulsen, T. Andersen, R. D. Cowan, P. Dahl, J. E. Hansen, and J. Engholm Pedersen, J. Phys. B **23**, 457 (1990).
[6] F. Penent, R. L. Champion, L. D. Doverspike, V. A. Esaulov, J. P. Grouard, R. I. Hall, and J. L. Montmagnon, J. Phys. B **21**, 3375 (1988).
[7] T. Andersen, P. Dahl, J. E. Hansen, J. Poulsen, and N. B. Thoft, J. Phys. B **22**, L591 (1989).
[8] J. S. Risley, in *Atomic Physics 6*, edited by R. Damburg (Plenum, New York, 1979), p. 223.
[9] A. K. Edwards and D. L. Cunningham, Phys. Rev. A **8**, 168 (1973); A. K. Edwards, J. S. Risley, and R. Geballe, *ibid.* **3**, 583 (1971).
[10] D. Spence and W. A. Chupka, Phys. Rev. A **10**, 71 (1974); D. Spence, *ibid.* **12**, 721 (1975).
[11] J. J. Matese, S. P. Rountree, and R. J. W. Henry, Phys. Rev. A **7**, 846 (1973).
[12] R. L. Chase and H. P. Kelly, Phys. Rev. A **6**, 2150 (1972).
[13] H. Hotop and W. C. Lineberger, J. Chem. Phys. Ref. Data **14**, 732 (1985); D. M. Newmark, K. R. Lykke, T. Andersen, and W. C. Lineberger, Phys. Rev. A **32**, 1890 (1985).
[14] P. Dahl, M. Rødbro, B. Fastrup, and M. E. Rudd, J. Phys. B **9**, 1567 (1976).
[15] R. D. Cowan, *The Theory of Atomic Structure and Spectra* (University of California Press, Berkeley, 1981), Chap. 8 and 16.
[16] C. Froese Fischer and T. Brage, Comput. Phys. Commun. **74**, 381 (1993).
[17] C. Froese Fischer, Comput. Phys. Commun. **64**, 369 (1991).
[18] C. Froese Fischer, Comput. Phys. Commun. **64**, 431 (1991).
[19] B. Cleff and W. Mehlhorn, J. Phys. B **7**, 593 (1974); J. Eichler and W. Fritsch, *ibid.* **9**, 1477 (1976); W. Mehlhorn and K. Taulbjerg, *ibid.* **13**, 445 (1980).
[20] K. Blum, *Density Matrix Theory and Applications* (Plenum, New York 1981).
[21] K. B. S. Eriksson, Ark. Fys. **30**, 199 (1965).
[22] J. Østgaard Olsen and N. Andersen, J. Phys. B **10**, 101 (1977).
[23] R. E. Huffman, J. C. Larrabee, and Y. Tanaka, J. Chem. Phys. **47**, 856 (1967); H. P. Palenius, Ark. Fys. **39**, 425 (1969); J. E. Hansen and W. Persson, Phys. Scr. **8**, 197 (1973).
[24] P. van der Meulen, M. O. Krause, C. D. Caldwell, S. B. Whitfield, and C. A. de Lange, Phys. Rev. A **46**, 2468 (1992).